Vietnam Journal of Science and Technology
DOI: https://doi.org/10.15625/2525-2518/20417

Synthesis and evaluation of carbon-based solid catalyst from sugar bagasse biochar for selective conversion of fructose to 5-HMF

Vu Nam Trung, Vu Tue Minh, Truong Duc Duc*, Le Quang Dien, Nguyen Trung Thanh, Tran Thi Thuy*

Hanoi University of Science and Technology, 1 Dai Co Viet Street, Bach Mai Ward, Ha Noi, Viet Nam

*Emails: 1: *duc.truongduc@hust.edu.vn*; 2: *thuy.tranthi3@hust.edu.vn*

Received: 22 March 2024; Accepted for publication: 18 July 2024

Abstract. A carbon-based solid acid catalyst was prepared from sugar bagasse by calcination of raw material and subsequent sulfonation step. The solid acid catalyst was characterized by XRD, TPD-NH3, FT-IR, and BET. Results showed that the catalyst has an amorphous carbon structure with surface area of above 750 m^2/g, acid density of approximately 10.65 mmol/g and strong acid sites of $-SO_3H$. XPS analysis showed high content of functional groups on the surface of the catalyst. 5-HMF was synthesized from fructose using the catalyst. Influence of reaction time on fructose conversion and 5-HMF selectivity was investigated. At reaction time of 2.5 h, 100 % of fructose was converted to 5-HMF with selectivity of 93.22 %.

Keywords: 5-HMF, carbon-based solid acid catalyst, fructose, sugar bagasse.

Classification numbers: 2.1.3.

1. INTRODUCTION

5-hydroxymethylfurfural (5-HMF) is one of the promising biomass-derived platforms [1–4]. This compound can be used to synthesize 2,5-furandicarboxylic acid (FDCA), a potential renewable crosslinker consisting of a furan ring at its core and two carboxylic acid groups. FDCA has garnered notable attention as a viable substitute for the widely used petrochemical monomer terephthalic acid (TPA) in the production of comparable biobased polymer [5]. Additionally, 5-HMF finds another application in the production of polyethylene 2,5-furandicarboxylate (PEF) as a replacement for the commonly employed petroleum-based polymer, polyethylene terephthalate (PET), serving the same purpose [6].

Generally, the synthesis of 5-HMF from sugar is a dehydration process aided by acid catalysts. The acid-catalysed triple dehydration of fructose is considered the most convenient synthetic method for producing 5-HMF. Among various starting materials, fructose offers advantages in 5-HMF production due to the higher reactivity of its fructofuranoic structure towards dehydration. Consequently, fructose is commonly employed as an ideal model substrate for evaluating the performance of catalytic systems in biomass conversion [7–9].

UNCORRECTED PROOF

There are many studies using fructose as a raw material for 5-HMF synthesis because of high 5-HMF yields and selectivity [10–13]. Combined with the isomerization of glucose to fructose, a two-stage synthesis of 5-HMF is potentially more efficient than direct synthesis of 5-HMF due to higher abundance and significantly cheaper price of glucose compared to fructose [14, 15].

The synthesis of 5-HMF initiates with the removal of one or two water molecules from fructose, resulting in partially dehydrated intermediates. These intermediates undergo further dehydration to yield the desired product. However, it is important to note that intermolecular reactions involving these intermediates can lead to the formation of undesired by-products, such as polymers and humins. Additionally, the rehydration of 5-HMF can result in the formation of levulinic acid. Therefore, the design of an efficient catalyst that promotes the dehydration of partially dehydrated intermediates while suppressing the hydrolysis of 5-HMF is of paramount importance in 5-HMF synthesis.

Recently, researchers have focused on exploring and utilizing solid acid catalysts for the dehydration process. Regarding the preparation methods, utilizing biomass as a renewable, abundant, and cost-effective resource offers potential advantages for the direct production of carbon-based solid acid catalysts. These includes good reusability, non-causticity, environmental friendliness, and production from renewable lignocellulosic material sources [11, 12, 16]. In comparison to alternative solid acids, CBSC offer distinct benefits that include facilitating streamlined processes for product separation and purification, minimizing the generation of waste, and alleviating concerns relating to catalyst disposal and equipment corrosion. Moreover, in terms of CBSC applications, the utilization of high surface area and porous carbon materials of various diameters facilitates enhanced contact between reactants and catalytic active sites, resulting in high catalytic activity and catalytic selectivity [11, 12, 17–20]. Besides, it is imperative to conduct further investigations aimed at enhancing the catalytic stability and mechanical strength of CBSC.

Huang and colleagues successfully demonstrated the efficient room-temperature conversion of microalgae lipids to biodiesel with a remarkable yield of 96.8 % [21]. This achievement was made possible through the utilization of a newly developed biomass-derived SO3H-functionalized graphene-like photothermal catalyst, known as S-NGL-600, under light irradiation. Significantly, the photothermal catalyst exhibited outstanding recyclability and outperformed the industrially used catalyst H_2SO_4 in terms of microalgae lipid conversion rate. Furthermore, a life cycle assessment revealed the energy-saving benefits (0.87 MJ/MJ) and environmental advantages (-89.42 CO_2eq/MJ) of the photothermal-driven approach for microalgae biodiesel production.

In a separate investigation conducted by Huang *et al.*, a layered 3D structure PAP-MEPP-C biochar catalyst with controllable acidity was synthesized through low-temperature carbonization (80 °C) of monomers derived from lignin [22]. The developed PAP-MEPP-C biochar catalyst exhibited notable catalytic activity in the conversion of Jatropha oil with varying acid values ranging from 17.9 to 155.4 mg KOH/g. This exceptional performance was attributed to the unique layered 3D structure and abundant acidity (5.33 mmol g^{-1}) from the -SO_3H groups, which facilitated optimal contact (174.4 m^2 g^{-1}) between reactants and acid sites. The study achieved a remarkable maximum biodiesel yield of 97.2 %. Furthermore, the investigated biochar catalyst exhibited high stability, allowing for four consecutive recycling cycles with a biodiesel yield exceeding 90 %.

UNCORRECTED PROOF

Charinpanitkul and co-authors synthesized sulfonated magnetic carbon nanoparticles (SMCN) from eucalyptus oil [11]. Experimental results showed 84 % fructose conversion rate with 51.6 % 5-HMF yield at reaction temperature of 180 °C, reaction time of 30 mins and catalyst to fructose mass ratio of 0.167. SMCN catalysts exhibit the ability to sustain their catalytic efficiency for up to three cycles without experiencing a notable decline. The environmentally conscious synthesis of SMCNs from renewable carbon feedstock, coupled with their impressive reusability, has the potential to facilitate the eco-friendly production of platform chemicals. However, high-temperature reactions in this work pose disadvantages related to the formation of humic substances. These by-products attach to the catalyst surface in the presence of water and thus leading to a decrease in catalyst activity and catalyst reuse [23, 24].

Douyong Min and associates prepared lignin-based carbon solid acid catalyst via sulfonation of lignin-based activated carbon solid with sulfuric acid [12]. At the recorded optimum conditions (reaction temperature of 170 °C, reaction time of 60 mins, catalyst dosage of 30 mg/mL, fructose concentration of 20 mg/mL), the yield of 5-HMF was 75.7 % in dimethyl sulfoxide media. After undergoing five consecutive recycling cycles, the catalyst demonstrated a noteworthy recovery rate surpassing 95 %, while achieving a yield of 5-HMF exceeding 70 %. This outcome carries substantial implications for cost reduction of catalysts and mitigation of environmental pollution, as the process excludes the utilization of mineral acid catalysts. In this work, XPS was used to characterize the catalyst. However, XPS was solely used to confirm the successful sulfonation process without considering the surface functional groups possibly present in the catalyst.

In our previous work, CBSC was prepared from acacia mangium wood sawdust via H_3PO_4 impregnation followed by sulfonation [25]. Under the optimized conditions, the obtained amount of catalyst was roughly 5.08 mmol/g of total acid site density and 740 m^2g^{-1} of specific surface area. Catalyst characterization by FT-IR method showed the formation of surface functional groups such as -OH, -COOH and C=O groups. The presence of these oxygen functional groups created hydrophilicity for the hydrophobic carbon structure of porous carbon and CBSC material, which promoted reactant access to $-SO_3H$ active sites while preventing the immediate poisoning of catalyst [26]. In addition, the weak and strong acidity of these groups also leaded to the effective catalytic performance of the CBSCs. However, the used FT-IR analysis method only confirmed the presence of the oxygen functional groups without quantifying the oxygen functional groups in the CBSC samples.

Numerous publications have reported on the utilization of carbon solid acid catalysts for the synthesis of 5-HMF [27–30], whose notable advantages arise from the presence of surface oxygen groups, which confer hydrophilic characteristics to the catalyst and facilitate the efficient dispersion of the active species onto the $-SO_3H$ sites. This enhanced dispersion significantly accelerates the desired reaction. The previous publications solely employed FT-IR analysis to confirm the presence of surface oxygen groups, predominantly -HSO3 groups, without quantifying them [27, 28, 30], while some others utilized XPS analysis to confirm the presence of particular specialized functional groups [27].

This study focuses on the preparation of CBSC from sugar bagasse as a catalyst for the selective conversion of fructose into 5-HMF. The synthesis process involved impregnating the sugar bagasse with an acidic aqueous solution, followed by carbonization to obtain CBSC. The catalytic performance of the CBSC in the conversion of fructose to 5-HMF was evaluated using temperature-programmed desorption of ammonia (TPD-NH3) analysis to determine the catalyst's acidity. The structural characterization of the carbon material and catalyst was conducted through X-ray diffraction (XRD) and Fourier Transform Infrared (FT-IR) Spectroscopy. X-ray

UNCORRECTED PROOF

photoelectron spectroscopy (XPS) was employed to investigate surface functional groups, while the catalyst's performance in the 5-HMF synthesis reaction was assessed using high performance liquid chromatography (HPLC) and gas chromatography–mass spectrometry (GC–MS). Notably, the innovative aspect of this study lies in the quantitative analysis of surface oxygen groups using XPS, which provides valuable insights into their abundance and facilitates a deeper understanding and advancement of this research area.

2. MATERIALS AND METHODS

2.1. Materials

Air-dried sugar bagasse was collected from Lam Son Sugar Cane Joint Stock Corporation, Thanh Hoa, Viet Nam. The material was stored in sealed containers at room temperature for experiments.

D-(-)-Fructose (CAS: 57-48-7, ≥ 99 wt%), phosphoric acid (CAS: 7664-38-2, ≥ 85 wt%), sulfuric acid (CAS: 7664-93-9, 98 %), DMSO (CAS: 67-68-5, ≥ 99.9 %), and other chemicals used in analytical methods were purchased from Sigma-Aldrich. All reagents were of analytical grade and utilized without further treatment.

2.2. Methods

2.2.1. Preparation of catalysts

The carbon-based solid acid catalysts were synthesized according to previous work with some modifications [25]. Typically, 100 g of the sugar bagasse was impregnated with 300 mL of 25 % w/w H_3PO_4 aqueous solution at 50 °C for 30 mins. After impregnation, pretreated sugar bagasse was separated from residual liquor and air-dried. The obtained solid product was then carbonized under argon flow to produce a carbon powder sample in a tube furnace. Typically, the sample was first heated from 25 to 450 °C at a heat increment of 2.0 °Cmin^{-1}, then the pyrolysis temperature was held at 450 °C for 1 h. The carbon material was obtained and ground to powder, and then washed by hot water to neutral pH. After washing, the carbon material was dried in oven at 105 °C.

In the sulfonation step, 10 g of the carbon material was heated in 50 mL of concentrated H_2SO_4 (98 %) at 100 °C in closed flask. After heating for 5 h and then cooling with ice, the cooled mixture was added to 400 mL of distilled water. The precipitate was washed repeatedly with hot distilled water until the filtrate becomes neutral. The precipitate was dried in an oven at 105 °C.

2.2.2. Catalyst characterization

Surface area, pore size distribution, average pore radius, and total pore volume of the solid acid catalysts (0.1 g sample size) were measured by N_2 adsorption and desorption using Gemini VII 2390 Surface Area Analyzer and Micromeritics ASAP 2020 V4.03. All samples were degassed under 120 °C to prevent samples burning.

Ammonia temperature-programmed desorption 2920 Analyzer was used to determine acid density of the catalysts. All samples were degassed by helium under 120 °C before Temperature-programmed desorption of ammonia (TPD-NH_3) analysis to prevent samples burning.

Structure of the carbon material and catalyst was determined by X-ray diffraction (XRD) and Fourier Transform Infrared (FT-IR) Spectroscopy. The powder XRD patterns were collected

UNCORRECTED PROOF

using Cu-Kα as radiation source (λ = 0.1540 nm) at an accelerating voltage of 40 kV and the current of 30 mA at the range of 2θ = 5-80°. FT-IR spectrum was obtained on a FT-IR 6700 NRX Raman Module- Thermo Nicolet. The frequency region between 4000 ÷ 400 cm^{-1} was examined.

X-ray photoelectron spectroscopy (XPS) was carried out on ESCALAB 250Xi (Thermo Fisher Scientific, USA) under an Al Ka X-ray irradiation. The semi quantitative analysis of narrow sweeping elements was adopted, and the binding energy was calibrated to the C_{1s} peak at 284.8 eV.

2.2.3. Conversion of fructose into 5-hydroxymethylfurfural

Typically, 1 g of fructose was dissolved in 10 mL DMSO in a 50 mL glass flask with a reflux condenser and a magnetic stirrer, 50 mg of sugar bagasse CBSC was then added to achieve 5 wt% of the catalyst dosage compared to fructose. The reaction was carried out in a constant temperature glycerol bath at 100 °C from 0.5 to 4 h, at stirring speed of 350 rpm. After reaction, the mixture was cooled to room temperature and then filtered by filter paper to separate liquid and the catalyst. The obtained liquid was then filtered by syringe filter 0.2 µm (Thermo Scientific™ F251317).

The 5-HMF content in the liquid was quantified by high performance liquid chromatography (HPLC) (Agilent 1200) with an Ultraviolet Detector at 284 nm (Agilent Eclipse XDB-C18 column). The column oven temperature was 25 °C, and the mobile phase was methanol/water (20/80 v/v) at a flow rate of 0.6 ml/min. The Agilent 2D LC ChemStation Software (G2170BA) was used for the analysis. The catalyst was washed repeatedly with hot distilled water then dried in an oven at 105 °C to recycle.

The fructose conversion was calculated from the initial amount of fructose and the amount of fructose remaining in the mixture after reaction. The selectivity of 5-HMF was calculated by the theoretical quantity of 5-HMF assuming that the consumed fructose was completely converted to 5-HMF and the actual quantity of 5-HMF in the mixture.

The gas chromatography–mass spectrometry (GC–MS) method was also used to analyse the obtained liquid after reaction.

3. RESULTS AND DISCUSSION

3.1. Catalyst characterization

3.1.1. XRD and BET

The specific surface areas and total pore volumes of the carbon materials and the catalyst are summarized in Table 1. The carbon-based solid acid catalysts with specific surface area lower than 2 m^2g^{-1} showed poor catalytic activities [31]. Therefore, this research was focused on the catalyst preparation from sugar bagasse with high specific surface area to ensure good accessibility to active sites. Obtained carbon material from carbonization without previous H_3PO_4 impregnation had very low specific surface area (1.79 m^2g^{-1}). Compared to nonactivated carbon material, the activated sample had higher specific surface areas (793.52 m^2g^{-1}). After sulfonation, the surface area of carbon material decreased from 793.52 to 754.19 m^2g^{-1}. The observed decrease in the surface area of the catalyst, compared to activated carbon, can be attributed to the carbon deposition process followed by -SO_3H functionalization. This process led to the occupation of some of the vacant pores within the catalyst. Meanwhile, the total pores volume decreased from 0.268 to 0.060 cm^3g^{-1}, which was potentially a result of the changes in pore diameter during sulfonation (from 3.0-9.3 nm to 2.5-2.9 nm). This phenomenon could be attributed to the higher

UNCORRECTED PROOF

degree of carbonization and the thinning of macropore walls at elevated temperatures, which can lead to the susceptibility of certain macropores to collapse. Besides, the collapse of specific macropores resulted in the formation of additional voids between the fragmented sections, thus lowering the total pore volume.

Table 1. Specific surface areas and total pore volumes of the carbon materials and the catalyst.

Sample	Specific surface area (m^2g^{-1})	Total pore volume (cm^3g^{-1})	Pore diameter (nm)
Nonactivated carbon	1.79	0.006	14.9-115.6
H_3PO_4 activated carbon	793.52	0.268	3.0-9.3
Catalyst	754.19	0.06	2.5-2.9

The N_2 isotherms linear plots of the carbon materials before and after sulfonation are shown in Figures 1 and 2, both have hysteresis loops in the relative pressure range of about 0.4-1, which is type IV, typical for mesoporous materials. However, the carbon material after sulfonation shows more microporous material specificity, evident from the similarity to the H4 hysteresis loop depicted in Figure 2.

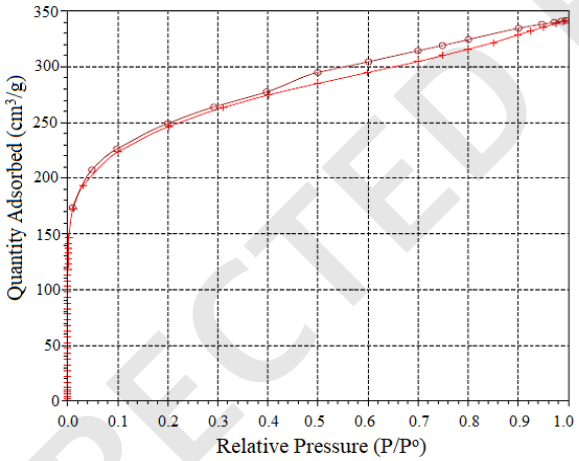

Figure 1. N_2 adsorption isotherm linear plot of the activated carbon material.

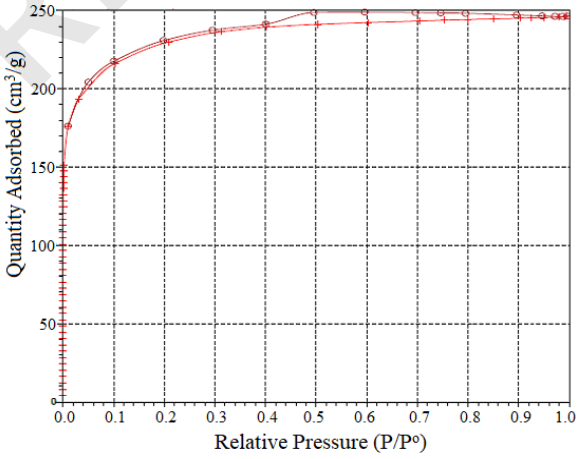

Figure 2. N_2 adsorption isotherm linear plot of the catalyst.

UNCORRECTED PROOF

Figure 3 shows XRD patterns of the carbon material and the catalyst. This indicates that the materials are amorphous carbon structures with the broad C (002) diffraction peak at approximately 2θ = 24°.

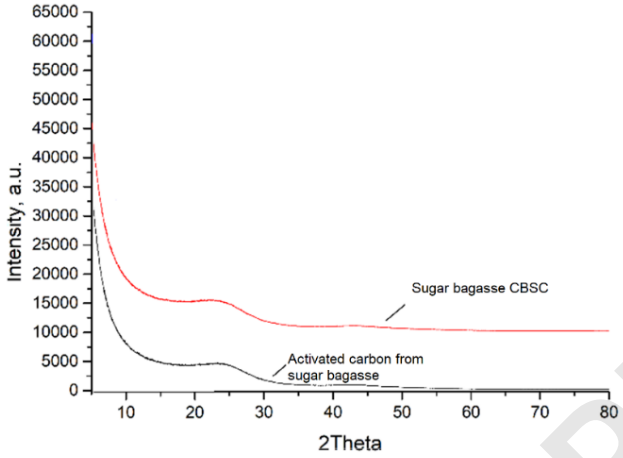

Figure 3. XRD patterns of the carbon material and the catalyst.

3.1.2. TPD-NH_3, FT-IR and XPS

Results of TPD-NH_3 analysis showed that the acidity of as-obtained catalyst samples was 10.65 mmol/g of total acid site density, including 0.63 mmol.g^{-1} of super strong acid site (897.6 °C), 8.45 mmol.g^{-1} of very strong acid site (526.6 °C), 1.29 mmol.g^{-1} of strong acid site (386.9 °C) and 0.28 mmol.g^{-1} of weak acid site (170 °C) (Figure 4). Compared to other published carbon-based solid acid catalyst [12, 20, 25, 32–35], the obtained catalyst in this work had much higher acid site density.

The acid sites of sulfonated carbon-based catalyst were contributed by -SO_3H, -COOH and -OH groups, which can be observed by FT-IR spectroscopy. The FT-IR spectra of the catalyst is shown in Figure 5. The peaks around 1035 cm^{-1} correspond to -SO_2 symmetric and 1176 cm^{-1} correspond to -SO_2 asymmetric stretching vibrations of -SO_3H [33]. This indicates that -SO_3H groups had successfully attached to the activated carbonized materials via sulfonation. The bands at around 3135 cm^{-1} the spectra assign to stretching vibrations of –OH groups in –COOH or phenolic compounds. In addition, the peaks at 1707 cm^{-1} are attributed to C=O stretching vibration.

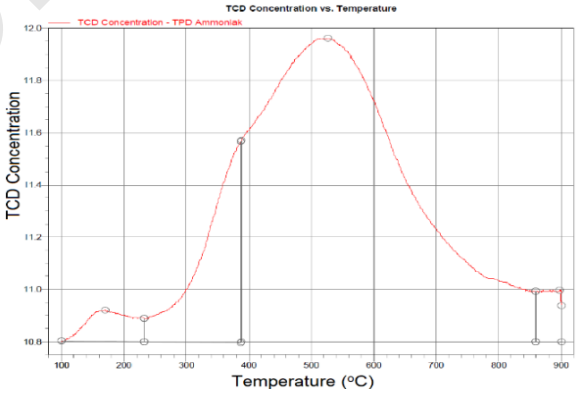

Figure 4. TPD-NH_3 analysis of the catalyst.

UNCORRECTED PROOF

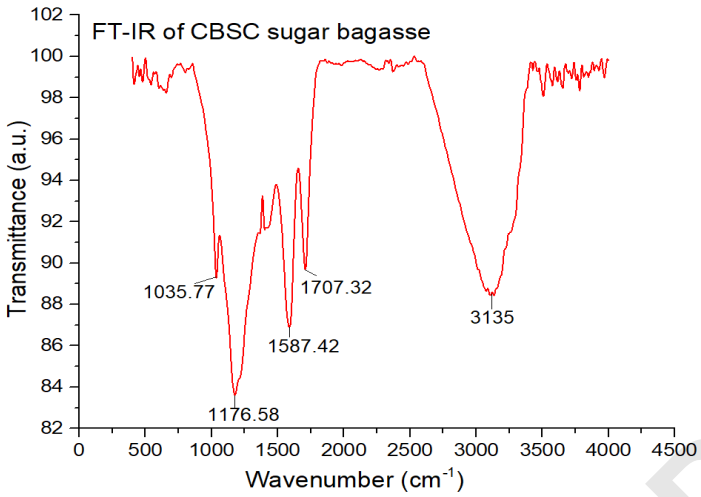

Figure 5. FT-IR spectra of the catalyst.

Under the same preparation conditions, both the catalyst sample from sugar bagasse in this work and the catalyst sample from wood sawdust in our previous work had a high acid site density. However, there was a significant difference in quantity, 10.65 mmol.g^{-1} and 5.08 mmol.g^{-1}, respectively. This indicates a difference in the surface functional group content of the catalysts.

XPS analysis was used to obtain a quantitative observation of the functional groups present in the catalyst samples. The XPS results of samples were shown in Figure 6 and content of functional groups listed in Table 2. The peaks were deconvoluted using Casa XPS software (v.2.3.15 rev1.3), and the content of functional groups was calculated by deconvolution of the C 1s XPS spectra.

For all the CBSC samples C 1s spectra resolved into five individual component peaks (Figures 6c and 6d), including C-C and/or C=C at 284.2–284.6 eV, C-O of phenols, ethers or alcohols at 285.8–286.4 eV, C=O of carbonyls, quinones at 287.0–287.4 eV, carboxylic groups at 288.6–289.0 eV and C-SO_3H at 290.0-290.5 eV [32, 34, 35]. A single pick around 169eV appeared on XPS spectra of samples in Figures 6a and 6b confirmed the presence of SO_3H on the surface of CBSCs.

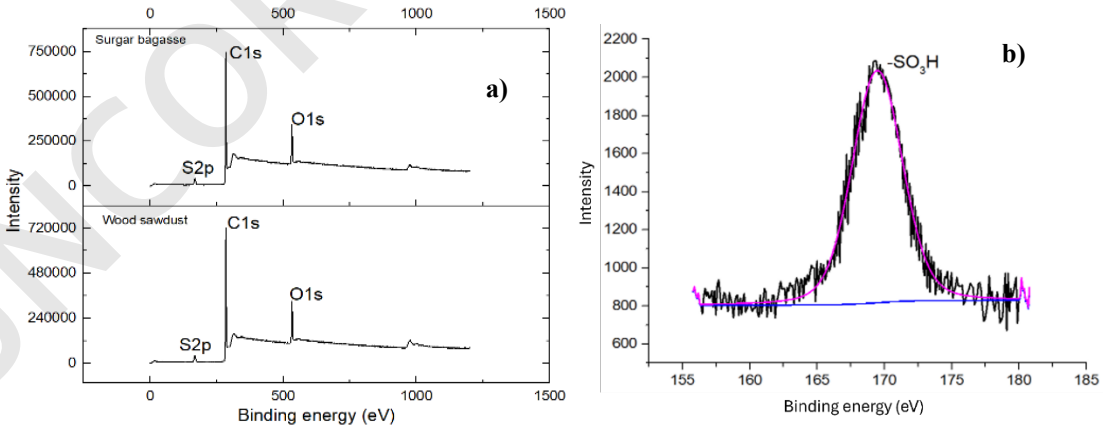

UNCORRECTED PROOF

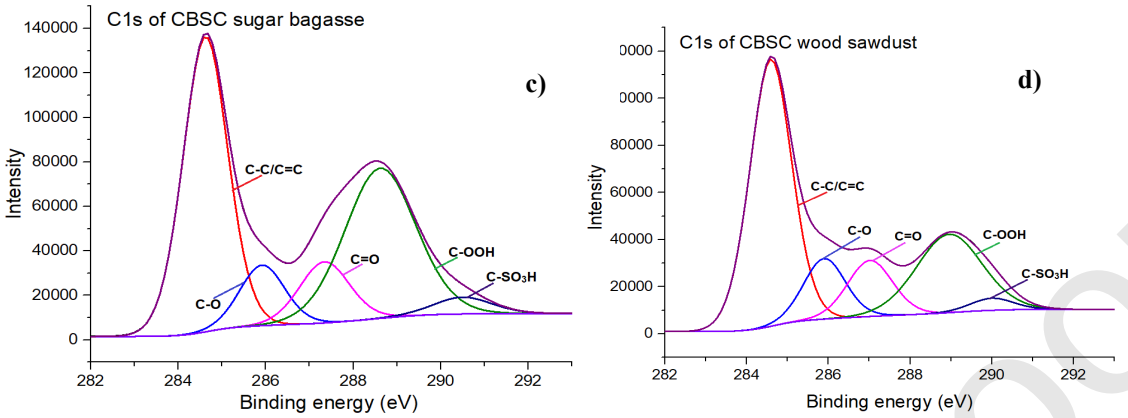

Figure 6. XPS spectra of sugarcane bagasse CBSC and wood sawdust CBSC (a), deconvoluted high-resolution S2p XPS spectra (b), C1s XPS spectra of sugarcane bagasse CBSC (c) and wood sawdust CBSC (d).

It is well known that oxygen functional groups such as phenol and carboxylic contribute to the acidity of CBSC catalyst. The results in Table 2 show negligible difference between the content of phenols, ethers, or alcohols groups of two catalysts, which explains the similarity of weak acid sites of the catalysts. The content of carboxylic group in sugarcane bagasse CBSC was 34.83 % and much higher than the concentration of 15 % in wood sawdust CBSC; the concentration of C-SO_3H group in sugarcane bagasse CBSC is also higher than in wood sawdust CBSC, 3.15 % and 2.37 %, respectively. These are consistent with the superior concentration of very strong acid sites of sugarcane bagasse CBSC over wood sawdust CBSC.

Table 2. The content of surface function group of CBSCs obtained from XPS method and acidity by TPD-NH_3 of sugarcane bagasse CBSC compared with wood sawdust CBSC from our previous work [25].

Component	Sugar bagasse CBSC				Wood sawdust CBSC			
	Peak position (eV)		Concentration (%)		Peak position (eV)		Concentration (%)	
C-C and/or C=C	284.62		43.13		284.59		51.06	
C-O	285.92		8.89		285.90		11.55	
C=O	287.34		9.99		287.02		11.53	
C-OOH	288.62		34.83		288.96		23.49	
C-SO_3H	290.50		3.15		290.00		2.37	
Quantity of acid sites (mmol.g^{-1})	Weak	Strong	Very strong	Super strong	Weak	Strong	Very strong	Super strong
	0.28	1.29	8.45	0.63	0.24	1.26	3.2	-

3.2. Fructose conversion

The catalytic conversion of sugars to 5-HMF is complicated due to side reactions, such as the formation of humic substances, and hydration of the 5-HMF into levulinic acid. High reaction temperatures can promote fructose conversion but will simultaneously decrease the 5-HMF selectivity. The fructose conversion at 170 °C was 98.0 % while 5-HMF selectivity was 75.7 %; at 180 °C fructose conversion was 84 % while 5-HMF selectivity was 51.6 % [11]. The formation of by-products such as humic substances also reduces the efficiency of catalyst reusability because these compounds adhere to the catalyst surface. In this work, the low-temperature conversion

UNCORRECTED PROOF

reactions were studied with the aim of preventing the formation of by-products and enhancing the yield of 5-HMF synthesis. In addition, this also contributes to a reduction in the energy expended in converting fructose to 5-HMF.

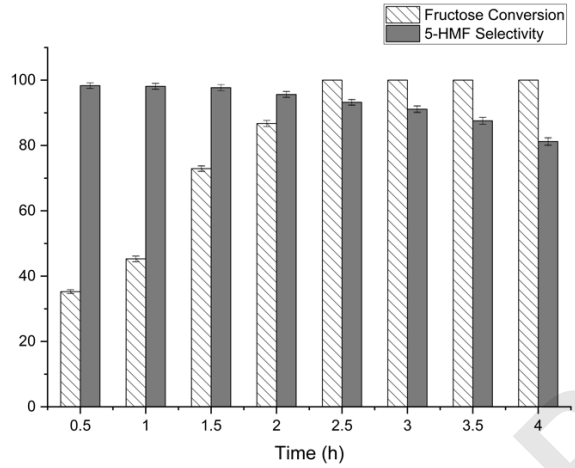

Figure 7. Fructose conversion and yield of 5-HMF selectivity at different reaction times.

The effects of the reaction time on the fructose conversion and yield of 5-HMF catalysed by acidic sugar bagasse biochar at 100 °C and catalyst dosage of 5 % was shown in Figure 7. The results show that with reaction time of 0.5 h, the conversion of fructose was 35.26 % and the fructose conversion increased with increasing reaction time; by reaction time of 2.5 h, 100 % of fructose was converted. With a reaction time of 0.5 h, the selectivity of 5-HMF was 98.34 % and the selectivity was inversely proportional to reaction time. After 4 h, the selectivity of 5-HMF was 81.22 %. Thus, when the reaction was conducted at low temperature (100 °C) and in DMSO media, the formation of by-products was minimized. The results also demonstrate that the obtained product 5-HMF can simultaneously converted to other products. With reaction time of 2.5 h, 100 % of fructose was converted with highest 5-HMF selectivity of 93.22 %. The underlying cause can be attributed to the significant surface area and large pore size of CBSC, facilitating the unrestricted movement of reactant and product molecules between the reaction solution and the catalyst surface.

Figure 8 shows GC-MS spectra of obtained liquid after reaction time of 2.5, 3.5, and 4 h. The number of by-products formed from 5-HMF increased when the reaction time was higher than 2.5 h.

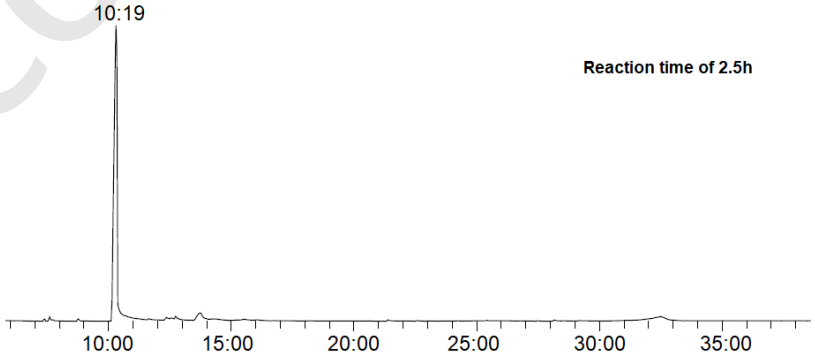

UNCORRECTED PROOF

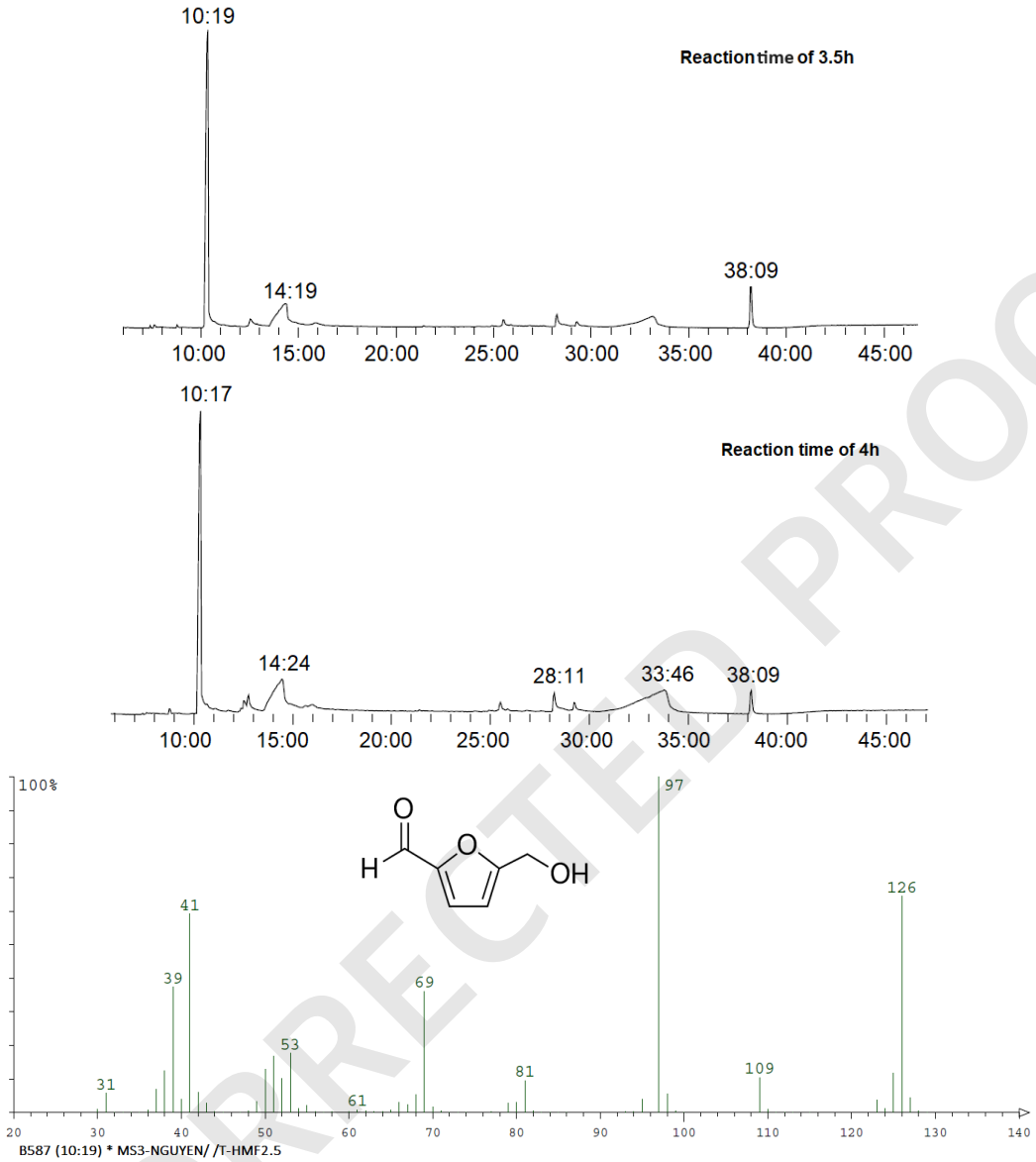

Figure 8. MS spectra of 5-HMF at different reaction times.

Table 3. Comparison of carbon solid catalyst properties and results.

Catalyst	Catalyst characterization				Conversion (%)	Selectivity (%)	Refs.
	-SO3H group (mmol.g^{-1})	S_{BET} (m^{2}g^{-1})	V_P (cm^{3}g^{-1})	D_s (nm)			
Sugar bagasse CBSC	10.65	754.19	0.06	2.5-2.9	100	93.22	This work
Wood sawdust CBSC	5.08	739.67	-	3-9.3	100	64	[25]
Sulfonated carbons with hierarchically	1.30	181	-	4.8	96.1	93.4	[30]

UNCORRECTED PROOF

ordered pores (SCHOP-500)							
Sulfonic acid-functionalized ordered mesoporous carbon	-	-	-	-	98.7	89.4	[29]
Carbon coated acid-activated red mud (AD-1:1/SO_3H)	6.8	69.23	-	6.84	93.05	51.5	[27]
Sulfonic acid-functionalized lignin-derived mesoporous carbon (LDM C-S O_3H)	-	261.7	0.067	3.42	100	98	[28]

4. CONCLUSIONS

A carbon-based solid acid catalyst was prepared from sugar bagasse. The catalyst had amorphous carbon structures with high specific surface area (754.19 m^2/g) and pore size distribution from 2.5 - 2.9 nm. The total acid site density of the catalyst of 10.65 $mmol.g^{-1}$ was contributed by -OH, -COOH and -SO_3H groups. The concentration of -COOH and -SO_3H groups was 34.83 % and 3.15 %, respectively.

The catalyst was applied to the dehydration of fructose into 5-HMF in DMSO solvent. The fructose was completely converted to 5-HMF with 93.22 % of selectivity at reaction parameters of 5 wt% catalyst loading, 2.5 h reaction time and 100 °C reaction temperature.

Acknowledgements. This research is funded by Hanoi University of Science and Technology under project number T2020-TD-204.

CrediT authorship contribution statement. Vu Nam Trung: Conceptualization, Methodology, Formal analysis, Writing – original draft. Vu Tue Minh: Conceptualization, Methodology, Formal analysis, Writing – original draft. Truong Duc Duc: Conceptualization, Writing – review & editing, Funding acquisition, Supervision. Le Quang Dien: Writing – review & editing, Supervision. Nguyen Trung Thanh: Writing – review & editing, Supervision. Tran Thi Thuy: Conceptualization, Writing – review & editing, Supervision.

Declaration of competing interest. The authors declare that they have no known competing financial interests or personal relationships that influence the work reported in this paper.

REFERENCES

1. Slak J., Pomeroy B., Kostyniuk A., Grilc M., Likozar B. – A review of bio-refining process intensification in catalytic conversion reactions, separations and purifications of hydroxymethylfurfural (HMF) and furfural. Chem. Eng. J., **429** (2022) 132325. https://doi.org/10.1016/j.cej.2021.132325.
2. Fan W., Verrier C., Queneau Y., Popowycz F. – 5-Hydroxymethylfurfural (HMF) in organic synthesis: a review of its recent applications towards fine chemicals. Curr. Org. Synth., **16** (2019) 583–614. https://doi.org/10.2174/1570179416666190412164738.
3. Kucherov F. A., Romashov L. V., Galkin K. I., Ananikov V. P. – Chemical transformations of biomass-derived C6-furanic platform chemicals for sustainable energy research, materials science, and synthetic building blocks. ACS Sustain. Chem. Eng., **6** (2018) 8064–8092. https://doi.org/10.1021/acssuschemeng.8b00971.

UNCORRECTED PROOF

4. van Putten R.-J., Van Der Waal J. C., De Jong E., Rasrendra C. B., Heeres H. J., de Vries J. G. – Hydroxymethylfurfural, a versatile platform chemical made from renewable resources. Chem. Rev., **113** (2013) 1499–1597. https://doi.org/10.1021/cr300182k.
5. Vu Trung N., Pham Thi N., Nguyen T. H., Nguyen M. N., Tran Anh D., Nguyen Trung T., Tran Quang T., Than Van H., Tran Thi T. – Tuning the thermal and mechanical properties of poly (vinyl alcohol) with 2, 5-furandicarboxylic acid acting as a biobased crosslinking agent. Polym. J., **54** (2021) 335–343. https://doi.org/10.1038/s41428-021-00583-y.
6. Vu Trung N., Nguyen Ngoc M., Nguyen Thi Ngoc A., Pham Thi N., Tran Quang T., Tran Thi T. – Synthesis and characterizations of biobased copolymer poly (ethylene-co-butylene 2, 5-furandicarboxylate). Int. J. Polym. Sci., **2021** (2021) 1–8. https://doi.org/10.1155/2021/9104546.
7. Amarasekara A. S., Williams L. D., Ebede C. C. – Mechanism of the dehydration of D-fructose to 5-hydroxymethylfurfural in dimethyl sulfoxide at 150 °C: an NMR study. Carbohydr. Res., **343** (2008) 3021–3024. https://doi.org/10.1016/j.carres.2008.09.008.
8. Assary R. S., Kim T., Low J. J., Greeley J., Curtiss L. A. – Glucose and fructose to platform chemicals: understanding the thermodynamic landscapes of acid-catalysed reactions using high-level *ab initio* methods. Phys. Chem. Chem. Phys., **14** (2012) 16603–16611. https://doi.org/10.1039/c2cp41842h.
9. Kimura H., Nakahara M., Matubayasi N. – Solvent effect on pathways and mechanisms for D-fructose conversion to 5-hydroxymethyl-2-furaldehyde: in situ ^{13}C NMR study. J. Phys. Chem. A, **117** (2013) 2102–2113. https://doi.org/10.1021/jp312002h.
10. Fu X., Li S., Wen J., Kang F., Huang C., Zheng X. – Visible light-induced photo-Fenton dehydration of fructose into 5-hydroxymethylfurfural over $ZnFe_2O_4$-coated Ag nanowires. Colloids Surf. A Physicochem. Eng. Asp., **609** (2021) 125685. https://doi.org/10.1016/j.colsurfa.2020.125685.
11. Le G. T., Arunaditya K., Panichpol J., Rodruangnon T., Thongratkaew S., Chaipojjana K., Faungnawakij K., Charinpanitkul T. – Sulfonated magnetic carbon nanoparticles from eucalyptus oil as a green and sustainable catalyst for converting fructose to 5-HMF. Catal. Commun., **149** (2021) 106229. https://doi.org/10.1016/j.catcom.2020.106229.
12. Li M., Zhang Q., Luo B., Chen C., Wang S., Min D. – Lignin-based carbon solid acid catalyst prepared for selectively converting fructose to 5-hydroxymethylfurfural. Ind. Crops Prod., **145** (2020) 111920. https://doi.org/10.1016/j.indcrop.2019.111920.
13. Rathod P. V., Mujmule R. B., Chung W.-J., Jadhav A. R., Kim H. – Efficient dehydration of glucose, sucrose, and fructose to 5-hydroxymethylfurfural using tri-cationic ionic liquids. Catal. Lett., **149** (2019) 672–687. https://doi.org/10.1007/s10562-019-02667-0.
14. Delidovich I. – Recent progress in base-catalyzed isomerization of D-glucose into D-fructose. Curr. Opin. Green Sustain. Chem., **27** (2021) 100414. https://doi.org/10.1016/j.cogsc.2020.100414.
15. Yabushita M., Shibayama N., Nakajima K., Fukuoka A. – Selective glucose-to-fructose isomerization in ethanol catalyzed by hydrotalcites. ACS Catal., **9** (2019) 2101–2109. https://doi.org/10.1021/acscatal.8b05145.
16. Lin F., Wang K., Gao L., Guo X. – Efficient conversion of fructose to 5-hydroxymethylfurfural by functionalized γ-Al_2O_3 beads. Appl. Organomet. Chem., **33** (2019) e4821. https://doi.org/10.1002/aoc.4821.
17. He Q., Lu Y., Peng Q., Chen W., Fan G., Chai B., Song G. – Synthesis of 5-hydroxymethylfurfural from fructose catalyzed by sulfonated carbon-based solid acid. Biomass Convers. Biorefin., **13** (2021) 9195–9203. https://doi.org/10.1007/s13399-021-01847-6.
18. Kang S., Ye J., Chang J. – Recent advances in carbon-based sulfonated catalyst: preparation and application. Int. Rev. Chem. Eng., **5** (2013) 133–144.
19. Karimi B., Mirzaei H. M., Behzadnia H., Vali H. – Novel ordered mesoporous carbon based sulfonic acid as an efficient catalyst in the selective dehydration of fructose into 5-HMF: the role of solvent and surface chemistry. ACS Appl. Mater. Interfaces, **7** (2015) 19050–19059. https://doi.org/10.1021/acsami.5b03985.
20. Wang Q., Hao J., Zhao Z. – Microwave-assisted conversion of fructose to 5-hydroxymethylfurfural using sulfonated porous carbon derived from biomass. Aust. J. Chem., **71** (2017) 24–31. https://doi.org/10.1071/CH17154.

UNCORRECTED PROOF

21. Huang J., Wang J., Huang Z., Liu T., Li H. – Photothermal technique-enabled ambient production of microalgae biodiesel: mechanism and life cycle assessment. Bioresour. Technol., **369** (2023) 128390. https://doi.org/10.1016/j.biortech.2022.128390.
22. Huang J., Jian Y., Li H., Fang Z. – Lignin-derived layered 3D biochar with controllable acidity for enhanced catalytic upgrading of *Jatropha* oil to biodiesel. Catal. Today, **404** (2022) 35–48. https://doi.org/10.1016/j.cattod.2022.04.016.
23. Kobayashi H., Fukuoka A. – Synthesis and utilisation of sugar compounds derived from lignocellulosic biomass. Green Chem., **15** (2013) 1740–1763. https://doi.org/10.1039/c3gc00060e.
24. Li X., Wang G., Hu Y., Iradukunda Y., Luo F., Yi K., Shi G. – Sulfonated carbon-titanium dioxide composite nanofiber tube catalysts for dehydration of sugars in biphasic solvents to obtain 5-hydroxymethylfurfural. J. Taiwan Inst. Chem. Eng., **129** (2021) 26–39. https://doi.org/10.1016/j.jtice.2021.09.025.
25. Thanh N. T., Long N. H., Dien L. Q., Phuong Ly G. T., Hoang P. H., Minh Phuong N. T., Hue N. T. – Preparation of carbonaceous solid acid catalyst from *Acacia mangium* wood sawdust for conversion of same source into 5-hydroxymethylfurfural. Energy Sources, Part A, **42** (2019) 730–739. https://doi.org/10.1080/15567036.2019.1602195.
26. Su F., Guo Y. – Advancements in solid acid catalysts for biodiesel production. Green Chem., **16** (2014) 2934–2957. https://doi.org/10.1039/C3GC42333F.
27. Das B., Mohanty K. – Sulfonic acid-functionalized carbon coated red mud as an efficient catalyst for the direct production of 5-HMF from D-glucose under microwave irradiation. Appl. Catal. A Gen., **622** (2021) 118237. https://doi.org/10.1016/j.apcata.2021.118237.
28. Gan L., Lyu L., Shen T., Wang S. – Sulfonated lignin-derived ordered mesoporous carbon with highly selective and recyclable catalysis for the conversion of fructose into 5-hydroxymethylfurfural. Appl. Catal. A Gen., **574** (2019) 132–143. https://doi.org/10.1016/j.apcata.2019.02.008.
29. Wang J., Zhang Z., Jin S., Shen X. – Efficient conversion of carbohydrates into 5-hydroxylmethylfurfan and 5-ethoxymethylfurfural over sufonic acid-functionalized mesoporous carbon catalyst. Fuel, **192** (2017) 102–107. https://doi.org/10.1016/j.fuel.2016.12.027.
30. Wang J. -g., Zhang Y. -y., Wang Y., Zhu L. -w., Cui H. -y., Yi W. -m. – Catalytic fructose dehydration to 5-hydroxymethylfurfural over sulfonated carbons with hierarchically ordered pores. J. Fuel Chem. Technol., **44** (2016) 1341–1348. https://doi.org/10.1016/S1872-5813(16)30058-5.
31. Fu Z., Wan H., Hu X., Cui Q., Guan G. – Preparation and catalytic performance of a carbon-based solid acid catalyst with high specific surface area. React. Kinet. Mech. Catal., **107** (2012) 203–213. https://doi.org/10.1007/s11144-012-0466-9.
32. Guan Q., Li Y., Chen Y., Shi Y., Gu J., Li B., Miao R., Chen Q., Ning P. – Sulfonated multi-walled carbon nanotubes for biodiesel production through triglycerides transesterification. RSC Adv., **7** (2017) 7250–7258. https://doi.org/10.1039/C6RA28067F.
33. Mardhiah H. H., Ong H. C., Masjuki H., Lim S., Pang Y. L. – Investigation of carbon-based solid acid catalyst from *Jatropha curcas* biomass in biodiesel production. Energy Convers. Manage., **144** (2017) 10–17. https://doi.org/10.1016/j.enconman.2017.04.038.
34. Wu Z.-Y., Yin P., Ju H.-X., Chen Z.-Q., Li C., Li S.-C., Liang H.-W., Zhu J.-F., Yu S.-H. – Natural nanofibrous cellulose-derived solid acid catalysts. Research (2019). https://doi.org/10.34133/2019/6262719.
35. Zhang T., Li W., Jin Y., Ou W. – Synthesis of sulfonated chitosan-derived carbon-based catalysts and their applications in the production of 5-hydroxymethylfurfural. Int. J. Biol. Macromol., **157** (2020) 368–376. https://doi.org/10.1016/j.ijbiomac.2020.04.148.

UNCORRECTED PROOF